Performance Analysis of 6TiSCH Networks Using Discrete Events Simulator

Guilherme de Santi Peron, Marcos Eduardo Pivaro Monteiro, João Luís Verdegay de Barros, Jamil Farhat and Glauber Brante

***Abstract*—The Internet of Things (IoT) empowers small devices to sense, react, and communicate, with applications ranging from smart ordinary household objects to complex industrial processes. To provide access to an increasing number of IoT devices, particularly in long-distance communication scenarios, a robust low-power wide area network (LPWAN) protocol becomes essential. A widely adopted protocol for this purpose is IPv6 over the time-slotted channel hopping (TSCH) mode of IEEE 802.15.4 (6TiSCH). It introduces TSCH mode as a new medium access control (MAC) layer operating mode, in conjunction with IEEE 802.15.4g, which also defines both MAC and physical layer (PHY) layers and provides IPv6 connectivity for LPWAN. Notably, 6TiSCH has gained adoption in significant standards such as Wireless Intelligent Ubiquitous Networks (Wi-SUN). This study evaluates the scalability of 6TiSCH, with a focus on key parameters such as queue size, the maximum number of single-hop retries, and the *slotframe* length. Computational simulations were performed using an open-source simulator and obtained the following results: increasing the transmission queue size, along with adjusting the number of retries and *slotframe* length, leads to a reduction in the packet error rate (PER). Notably, the impact of the number of retries is particularly pronounced. Furthermore, the effect on latency varies based on the specific combination of these parameters as the network scales.**

***Index Terms*—6TiSCH, TSCH, LPWAN, IoT.**

I. Introduction

EMPOWERED by sensing, communication, and computing capabilities, the Internet of Things (IoT) stands as a revolutionary technology that seamlessly bridges the physical and virtual worlds. Projections indicate that by 2030, approximately 80 billion IoT devices will be interconnected [1]. Leveraging advancements in communications, edge computing, and artificial intelligence, IoT has enabled a multitude of applications and services, including smart homes, agriculture, smart cities, and more [2], [3]. Within this context, a reliable low-power wide-area network (LPWAN) protocol is crucial for communication over long distances, as seen in scenarios like smart grid solutions [4]. Then, in this variety of application scenarios, IEEE 802.15.4g stands out as one very promising protocol stack. It utilizes the upper layers defined by IPv6 over the time-slotted channel hopping (TSCH) mode of IEEE 802.15.4 (6TiSCH), which is supported by the Internet Engineering Task Force (IETF). This long-range mesh protocol has been considered in various works [5]–[7].

Considering the extensive coverage of LPWA networks, each node faces the challenge of sharing the communication spectrum with numerous other communication devices. Despite various available strategies to mitigate interference, such as employing orthogonal configurations of center frequency, spreading factor (SF), and similar parameters, a limitation remains regarding the maximum feasible number of nodes within a designated area. This scalability issue of the 6TiSCH stack protocol has been investigated in [8], revealing that the 6TiSCH network experiences a significant impact in terms of packet error rate (PER) as the number of nodes increases. This impact is due to effects like collisions and full transmit queues of the IoT devices.

The network performance of IEEE 802.15.4 TSCH and 6TiSCH has been extensively studied in several works [8]–[14]. In [9], the authors investigate QoS in 6TiSCH networks within the context of Industrial IoT (IIoT) by the implementation of a CoAP-based solution for remote network and schedule management. Considering other scheduling schemes, [10] presents a low-latency autonomous scheme for 6TiSCH IIoT networks, while a real-time slot allocation scheme is proposed in [11] for highly dynamic network traffic. Finally, [12] develops a scheduling function that combines low-latency and machine-learning techniques to adapt to dynamic traffic changes.

In terms of performance evaluation, [13] assesses a standard-compliant 6TiSCH solution from the end-user perspective, providing indicators to determine its suitability. To enhance communication reliability, [14] proposes an optimization approach aimed at improving the successful delivery of emergency flows. Furthermore, [8] conduct an analysis of the scalability of 6TiSCH and LoRaWAN for LPWAN.

In this work, differently from [8], in which a comparison between LoRaWAN and 6TiSCH is performed, we investigate the impact of queue size, maximum single-hop retries, and *slotframe* length focusing on the scalability of the 6TiSCH stack protocol. To the best of our knowledge, this is the first work that explores such important parameters from a scalability perspective, which constitutes the novelty of this work and can help system designers to correctly project 6TiSCH networks for a particular set of scalability requirements. To

G.S. Peron (ORCID: 0000-0001-5794-0237) and J.L.V. Barros (ORCID: 0009-0000-0204-2798) are with Graduate Program in Energy Systems (PPGSE), Federal University of Technology - Paraná (UTFPR), Curitiba-PR, Brazil (e-mails: peron@utfpr.edu.br, barros.joao.luis@gmail.com). M.E.P. Monteiro (ORCID: 0000-0001-7658-2025) is with Academic Department of Electronics (DAELN), Federal University of Technology - Paraná (UTFPR), Curitiba-PR, Brazil (e-mail: marcose@utfpr.edu.br). J. Farhat (ORCID: 0000-0002-7525-4334) and G. Brante (ORCID: 0000-0001-6006-4274) are with Graduate Program in Electrical and Computer Engineering (CPGEI), Federal University of Technology - Paraná (UTFPR), Curitiba-PR, Brazil (e-mails: jamilfarhat@utfpr.edu.br, gbrante@utfpr.edu.br). This work has been partially supported by Agência Nacional de Energia Elétrica and Celesc Distribuição S.A. (PD05697-1323/2023).

Submission: 2024-04-25, First decision: 2024-06-17, Acceptance: 2024-10-09, Publication: 2024-10-21.

Digital Object Identifier: 14209/jcis.2024.18

obtain such results, the open source 6TiSCH Simulator [15] is employed to analyze the network. The results show that increasing the maximum number of single-hop transmission attempts exerts substantially more influence on system scalability than enlarging the transmission queue size. Additionally, we observe that increasing the transmission queue size can reduce both latency and PER when the *slotframe* is expanded.

II. System Model

We consider $\mathcal{N}$ nodes uniformly and randomly distributed in a square area of $\mathcal{D} \times \mathcal{D}$ km^2 that transmit messages to a root node at the center of the square, as shown in Fig. 1. All nodes operate in the license-free 915 MHz industrial scientific and medical (ISM) band to enable long-range transmissions and avoid frequency-related fees. The channel spacing is $\mathcal{S} = 200$ kHz, which is a common parameter for 802.15.4g using operating mode 1 for the US ISM (902-928 MHz) frequency band [16], which indicates a transmit rate of 50 kbps and filtered 2-Frequency-Shift Keying (FSK) modulation [16].

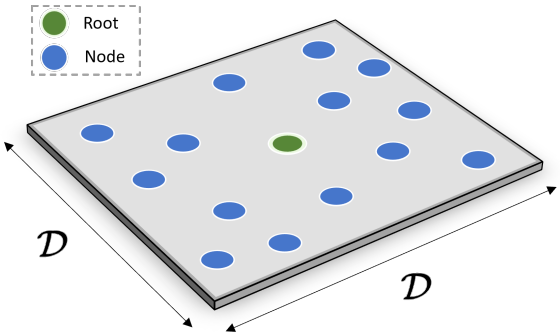

Fig. 1. System model with $\mathcal{N}$ nodes uniformly distributed in a square area of $\mathcal{D} \times \mathcal{D}$ km^2 with a root node at the center.

A 6TiSCH network is simulated using the 6TiSCH Simulator, similar to that performed in [8]. 6TiSCH networks enhance reliability and reduce interference through TSCH, which schedules communication times and channels and uses channel hopping to enhance robustness against interference and multipath fading. Each timeslot must be sufficiently long to accommodate both the frame and its subsequent acknowledgment. A sequence of $\mathcal{T}$ timeslots, referred to as a *slotframe*, is repeated cyclically.

The network also utilizes the Routing Protocol for Low Power and Lossy Networks (RPL), which adapts to topology changes by recalculating routes as needed and employing the default Objective Function Zero (OF0) implementation within the 6TiSCH Simulator to optimize multipoint-to-point routes. Finally, we use the minimum scheduling function to optimize the allocation of communication resources, efficiency, and reliability while also mitigating the interference within the network. The packet transmission rate per node follows a Poisson distribution, with an average rate of one packet every $t = 1$ minute. This configuration is similar to that described in [17] and mirrors scenarios observed in WirelessHART networks.

The received power, $\mathcal{P}_\mathrm{r}$, in dBm is defined as [18]

$$\mathcal{P}_\mathrm{r} = 10 \log_{10} \left(\frac{\mathcal{P}_\mathrm{t} \mathcal{G} \lambda^2}{(4\pi d)^2} \right), \tag{1}$$

employing the Friis model, where d is the link distance in meters, $\mathcal{P}_\mathrm{t} = 14$ dBm is the transmitted power[1], λ is the wavelength in meters, and $\mathcal{G} = \frac{\mathcal{G}_\mathrm{t}\mathcal{G}_\mathrm{r}}{L}$ is the gain associated with transmitting antenna ($\mathcal{G}_\mathrm{t}$), receiving antenna ($\mathcal{G}_\mathrm{r}$) and loss factor (L), which are all assumed to be unitary in this work.

We employ the Pister-Hack propagation model to account for long-term variations in transmission. In this model, the Received Signal Strength Indicator (RSSI) levels are fine-tuned to match with empirical results [20]. Specifically, we subtract a uniformly distributed variable ranging from 0 to 40 dB from the expression in (1). As a result, for a received power level of $\mathcal{P}_\mathrm{r} = -80$ dBm, the final RSSI spans from -80 dBm to -120 dBm. Interfering signals are treated as noise, and the RSSI is converted to the Packet Error Rate (PER) using [8, Table 1] to assess the success of the transmission. This RSSI-to-PER conversion follows the methodology described in [8], where a sensitivity level of -106.37 dBm corresponds to a PER of 1.0, with the PER decreasing as the RSSI exceeds this sensitivity threshold.

III. Results

In this section, we evaluate the performance of 6TiSCH under various network parameters. We focus on how the maximum retries, queue size, and *slotframe* length affect the PER and latency [2]. We consider two *slotframe* lengths: $\mathcal{T} = 101$ timeslots, with a slot duration of 0.04 s, which is the default in 6TiSCH [21], resulting in a *slotframe* of 4.04 s; and $\mathcal{T} = 606$ timeslots, with a slot duration of 0.04 s, resulting in a *slotframe* of 24.24 s. Consequently, the *slotframe*s repeat approximately every 4 s and 24 s, respectively, for $\mathcal{T} = 101$ and $\mathcal{T} = 606$. Additionally, we assume that $\mathcal{D} = 2$ km, and that $\mathcal{C} = 8$ channels are available, following the same assumption as Barros *et al.* [8].

Figs. 2 and 3 depict the PER as a function of the number of nodes ($\mathcal{N}$) for various combinations of *slotframe* length ($\mathcal{T}$) and queue size ($\mathcal{Q}$), while considering different values for the maximum number of retries, denoted as $\mathcal{R}$. As we observe, increasing both $\mathcal{N}$ and $\mathcal{T}$ results in a reduction in PER, leading to improved performance in both figures. Notably, from the results shown in Fig. 2 (with $\mathcal{R} = 2$), it is evident that increasing the *slotframe* length has a more pronounced impact on reducing PER compared to increasing the transmission queue. In addition, increasing the queue size 200 times, from $\mathcal{Q} = 10$ to $\mathcal{Q} = 2000$, resulted in a reduction of up to 1.52 times for $\mathcal{T} = 101$ and up to 12 times for $\mathcal{T} = 606$.

[1] $\mathcal{P}_\mathrm{t} = 14$ dBm is the maximum transmit power for many LPWAN microcontrollers [19], while also being the maximum output power allowed by the European Telecommunications Standards Institute (ETSI).

[2] The proposed system model is designed to optimize the 6TiSCH network, which implies a mesh communication. In contrast, other LPWA network alternatives, such as LoRaWAN, utilize a star topology for message transmission [8]. The parameters examined in this study are specific to the mesh network scenario. Consequently, the performed analysis does not apply to networks with different topologies, which are beyond the scope of this paper.

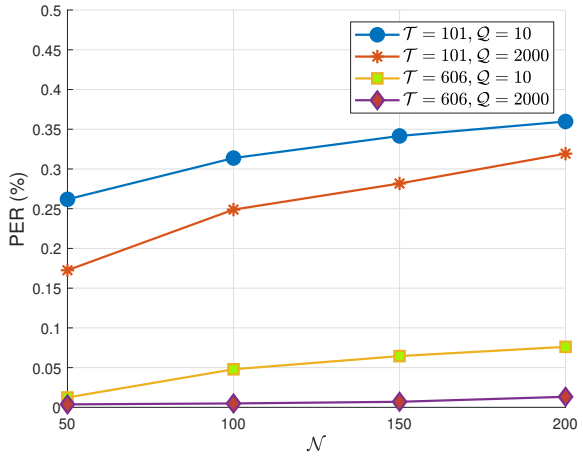

Fig. 2. PER as a function of $\mathcal{N}$ with $\mathcal{D} = 2$ km and different values of $\mathcal{Q}$, $\mathcal{T}$ and $\mathcal{R} = 2$.

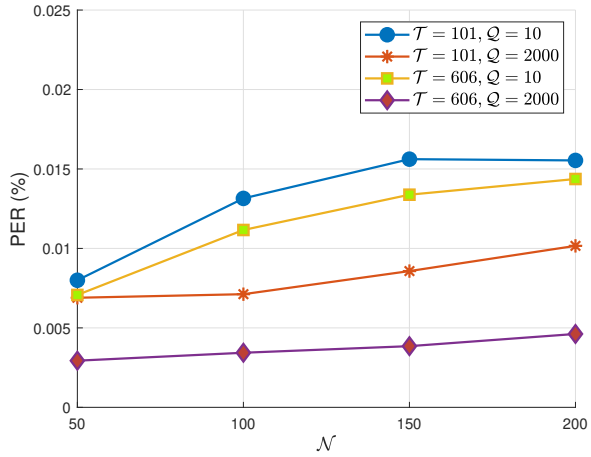

Fig. 3. PER as a function of $\mathcal{N}$ with $\mathcal{D} = 2$ km and different values of $\mathcal{Q}$, $\mathcal{T}$ and $\mathcal{R} = 200$.

Meanwhile, a sixfold increase in the *slotframe* length, from 101 to 606, led to a PER reduction of up to 21 times for $\mathcal{Q} = 10$ and up to 55 times for $\mathcal{Q} = 2000$. In general, a longer *slotframe* allows for a more extended scheduling period, which reduces the likelihood of overlapping transmissions and decreases contention among nodes. This results in fewer collisions and a lower PER. In contrast, increasing the queue size impacts the buffer capacity, allowing more packets to be queued and transmitted but not directly addressing collision issues.

Fig. 3 reveals that, with $\mathcal{R} = 200$, the queue size has a more pronounced impact on PER reduction than the *slotframe* length. This shift can be explained by the increased ability to handle more transmission attempts. An increased number of retries provides additional opportunities for successful packet retransmission, while a larger queue size eases more effective management of these retransmissions. Consequently, the impact of queue size on reducing PER becomes more pronounced. Specifically, increasing the queue size 200 times, from $\mathcal{Q} = 10$ to $\mathcal{Q} = 2000$, reduced the PER by up to 1.85 times for $\mathcal{T} = 101$ and up to 3.47 times for $\mathcal{T} = 606$. Furthermore, a six-unit increase in the length of the *slotframe*, from 101 to 606, resulted in a reduction of up to 1.18 times for $\mathcal{Q} = 10$ and up to 2.34 times for $\mathcal{Q} = 2000$ in PER. Additionally, similar to Fig 2, we verify that an increase in node density leads to higher PER values due to the increased probability of concurrent transmission among multiple devices. This demonstrates the paramount importance of appropriately choosing $\mathcal{T}$, $\mathcal{Q}$ and $\mathcal{R}$. Finally, comparing Figs. 2 and 3, we observe that increasing the number of retransmissions yields a more significant PER decrease. A higher retry count allows for additional chances to successfully transmit packets that may have failed initially due to collisions or any other issues, consequently contributing to a more considerable overall reduction in PER.

In the sequel, Fig. 4 analyzes the PER as a function of $\mathcal{N}$, with special focus on errors caused by the maximum number of retries being reached considering $\mathcal{R} = 2$. We notice that a *slotframe* length of $\mathcal{T} = 101$ exhibits a higher PER for the maximum number of retries. This is because, for $\mathcal{T} = 606$, there is a lower number of collisions, decreasing both the need for retransmission and the number of packets failing due to the retries limit. Additionally, it is noteworthy that this result indicates the potential occurrence of more losses related to transmission queues. Regarding the increase in the message queue from $\mathcal{Q} = 10$ to $\mathcal{Q} = 2000$, simulation results demonstrate a lower PER. This confirms that increasing the message queue influences transmission success in scenarios with an extended *slotframe* length.

Next, Fig. 5 analyzes the PER as a function of $\mathcal{N}$, with a specific focus on errors caused due to the full queue with $\mathcal{Q} = 10$. Notably, a lower full queue error rate is achieved with reduced $\mathcal{T}$ values. This behavior can be attributed to the fact that, with $\mathcal{T} = 101$, the frequency of errors due to reaching the maximum number of retries is higher than with $\mathcal{T} = 606$. However, as previously observed in Fig. 4, the increase in $\mathcal{T}$ contributes to a more efficient allocation and distribution of slots compared to $\mathcal{T} = 101$. Consequently, timely message transmission is facilitated by reducing errors due to the maximum number of retransmissions at $\mathcal{T} = 606$, albeit resulting in an accumulation of errors due to the full message queue. In a scenario with $\mathcal{T} = 606$, an increase in $\mathcal{R}$, as expected, reduces the error rate due to a full queue for both $\mathcal{T} = 101$ and $\mathcal{T} = 606$. Specifically, simulations with $\mathcal{R} = 200$ and $\mathcal{T} = 606$ exhibit a decrease of up to 19% in the full queue error rate compared to $\mathcal{R} = 2$ and $\mathcal{T} = 606$, which can be attributed to the additional number of retransmission attempts. Similarly, for simulations with $\mathcal{R} = 200$ and $\mathcal{T} = 101$, a reduction of up to 50% in the full queue error rate is observed compared to $\mathcal{R} = 2$ and $\mathcal{T} = 101$, further justified by the higher number of transmission attempts.

Finally, the results depicted in Fig. 6 illustrate the latency variation versus $\mathcal{N}$ when $\mathcal{T} = 101$. The figure reveals that an increase in $\mathcal{R}$ leads to a slight elevation in latency. This increase is due to the fact that, while allowing a greater number

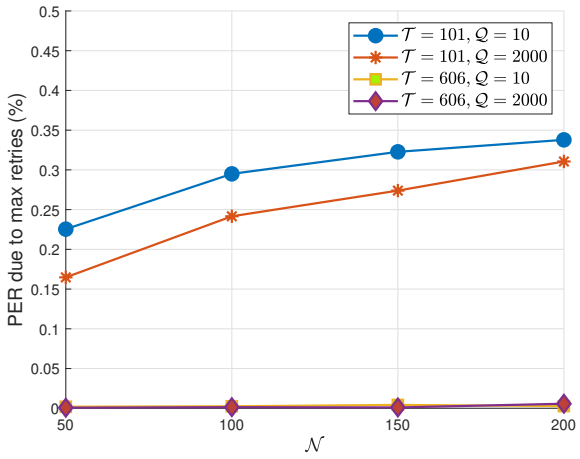

Fig. 4. PER due to maximum retries as a function of $\mathcal{N}$ with $\mathcal{D} = 2$ km and $\mathcal{R} = 2$.

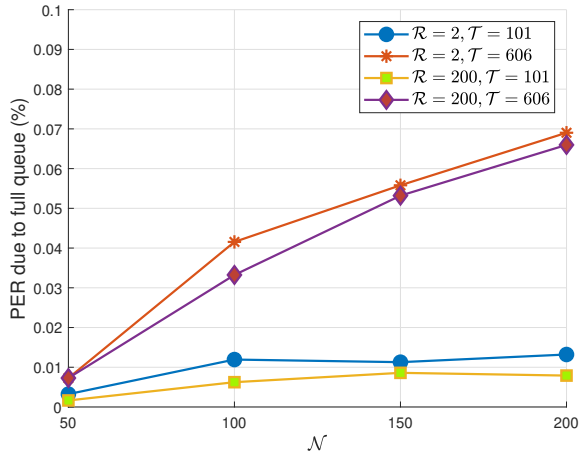

Fig. 5. PER due to full queue as a function of $\mathcal{N}$ with $\mathcal{D} = 2$ km and $\mathcal{Q} = 10$.

of single-hop retries diminishes the PER, it also means it may take longer to complete the multi-hop transmission. Specifically regarding $\mathcal{N}$, a lower node density with an enlarged queue size prevents unnecessary packet retransmissions while facilitating efficient slot allocation. However, as $\mathcal{N}$ increases, this efficient allocation diminishes, resulting in higher-latency packet delivery. It is worth mentioning that, nonetheless, the impact of a slightly increased latency depends on the application of the network. For instance, for systems with milder latency requirements, the increase in $\mathcal{Q}$ is usually beneficial since it reduces the PER. Furthermore, the variation in latency as a function of $\mathcal{N}$ when $\mathcal{T} = 606$ can be observed in Fig. 7. As depicted in Fig. 6, increasing $\mathcal{R}$ results in higher latency in Fig. 7, primarily due to the multiple-hop retransmissions inherent in the mesh topology. However, contrary to Fig. 6, latency decreases with increasing $\mathcal{Q}$ for all $\mathcal{N}$. This behavior is attributed to the larger *slotframe* length, which allows for more efficient utilization of the increased queue size, thus reducing latency. A larger *slotframe* length provides a broader time window for packet transmission and slot allocation, which mitigates the delays associated with packet retransmissions. For $\mathcal{T} = 101$ the maximum tree depth is 4 and 6 for, respectively, $\mathcal{N} = 50$ and $\mathcal{N} = 200$, and for $\mathcal{T} = 606$ the maximum tree depth is 6 and 8 for, respectively, $\mathcal{N} = 50$ and $\mathcal{N} = 200$, which justifies the increasing latency with $\mathcal{T}$.

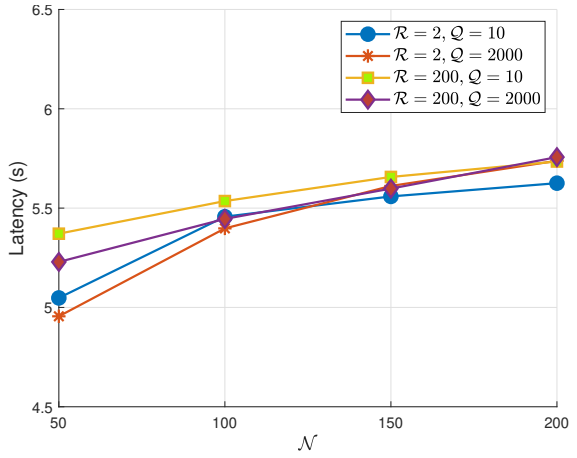

Fig. 6. Latency as a function of $\mathcal{N}$ for different values of $\mathcal{R}$ and $\mathcal{Q}$ with $\mathcal{D} = 2$ km and $\mathcal{T} = 101$.

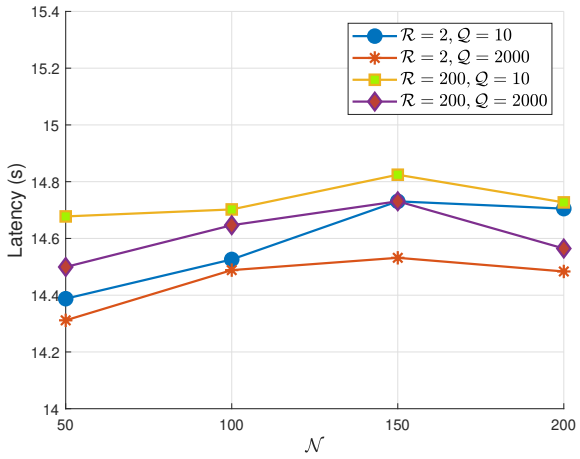

Fig. 7. Latency as a function of $\mathcal{N}$ for different values of $\mathcal{R}$ and $\mathcal{Q}$ with $\mathcal{D} = 2$ km and $\mathcal{T} = 606$.

IV. Conclusions

In this work, we investigated the influence of 6TiSCH parameters by varying three key factors: the maximum number of retries, the transmission queue size, and *slotframe* length. The results demonstrate that increasing the transmission queue size and the maximum number of retries leads to a reduction in terms of PER. However, it's worth noting that the impact of increasing the maximum retries is significantly more pronounced than that of increasing the transmission queue size. Furthermore, when the *slotframe* length is greater, increasing the transmission queue size is more effective in achieving both latency reduction and PER improvement. In contrast, for smaller *slotframe*, although both latency and PER decrease with fewer nodes, there is an increase in latency as the number of nodes grows.

REFERENCES

[1] L. Chettri and R. Bera, "A comprehensive survey on Internet of Things (IoT) toward 5G wireless systems," *IEEE Internet Things J.*, vol. 7, no. 1, pp. 16–32, 2020, doi: 10.1109/JIOT.2019.2948888.

[2] F. De Keersmaeker, Y. Cao, G. K. Ndonda, and R. Sadre, "A survey of public IoT datasets for network security research," *IEEE Commun. Surv. Tutor.*, vol. 25, no. 3, pp. 1808–1840, 2023, doi: 10.1109/COMST.2023.3288942.

[3] Z. Wang, D. Liu, Y. Sun, X. Pang, P. Sun, F. Lin, J. C. S. Lui, and K. Ren, "A survey on IoT-enabled home automation systems: Attacks and defenses," *IEEE Commun. Surv. Tutor.*, vol. 24, no. 4, pp. 2292–2328, 2022, doi: 10.1109/COMST.2022.3201557.

[4] L. F. Venturini, Y. L. Baracy, R. V. P. C. Silva, B. K. De Freitas, E. P. Dos Santos, N. O. Branco, M. E. P. Monteiro, J. F. Hübner, and D. Issicaba, "Balancing decentralization for restoration in power distribution systems with agents," *IEEE Access*, vol. 10, pp. 77 993–78 001, 2022, doi: 10.1109/ACCESS.2022.3192847.

[5] R. Yadav, R. Saroj, A. Kumar Verma, and A. Kumar Mishra, "A survey of IoT and machine learning based monitoring of the growth of crops using blockchain technology," in *Int. Conf. on IoT, Comm. and Autom. Tech. (ICICAT)*, 2023, pp. 1–7, doi: 10.1109/ICICAT57735.2023.10263755.

[6] L. S. Melo, F. L. Tofoli, D. Issicaba, M. E. P. Monteiro, G. C. Barroso, R. F. Sampaio, and R. P. S. Leao, "Co-simulation platform for the assessment of transactive energy systems," *Electr. Pow. Syst. Res.*, vol. 223, p. 109693, 2023, doi: https://doi.org/10.1016/j.epsr.2023.109693.

[7] K. T. Kim, H. Kim, H. Park, and S. Kim, "An industrial IoT MAC protocol based on IEEE 802.15.4e TSCH for a large-scale network," in *Int. Conf. on Advanced Commun. Technol. (ICACT)*, 2017, pp. 721–724, doi: 10.23919/ICACT.2017.7890187.

[8] J. L. V. de Barros, M. E. P. Monteiro, G. S. Peron, G. L. Moritz, O. K. Rayel, and R. D. Souza, "LoRaWAN vs. 6TiSCH: Which one scales better?" *Comput. Commun.*, vol. 184, pp. 1–11, 2022, doi: https://doi.org/10.1016/j.comcom.2021.12.004.

[9] M. Mohamadi, Q. Lampin, and M. Dumay, "CoAP-Based remote network management model for deterministic 6TiSCH networks," *IEEE Internet of Things Journal*, pp. 1–1, 2024, doi: 10.1109/JIOT.2024.343539.

[10] N. M. Pradhan, B. S. Chaudhari, and M. Zennaro, "6TiSCH low latency autonomous scheduling for Industrial Internet of Things," *IEEE Access*, vol. 10, pp. 71 566–71 575, 2022, doi: 10.1109/ACCESS.2022.3188862.

[11] A. Kalita and M. Gurusamy, "On-the-fly autonomous slot allocation in 6TiSCH-Based Industrial IoT networks," *IEEE Transactions on Industrial Informatics*, vol. 20, no. 7, pp. 9365–9374, 2024, doi: 10.1109/TII.2024.3385117.

[12] Y. H. Pratama, S.-H. Chung, and D. Z. Fawwaz, "Low-latency and Q-Learning-based distributed scheduling function for dynamic 6TiSCH networks," *IEEE Access*, vol. 12, pp. 49 694–49 707, 2024, doi: 10.1109/ACCESS.2024.3384869.

[13] M. Vučinić, T. Chang, B. Škrbić, E. Kočan, M. Pejanović-Djurišić, and T. Watteyne, "Key performance indicators of the reference 6TiSCH implementation in Internet-of-Things scenarios," *IEEE Access*, vol. 8, pp. 79 147–79 157, 2020, doi: 10.1109/ACCESS.2020.2990278.

[14] H. Farag, S. Grimaldi, M. Gidlund, and P. Österberg, "REA-6TiSCH: Reliable emergency-aware communication scheme for 6TiSCH networks," *IEEE Internet of Things Journal*, vol. 8, no. 3, pp. 1871–1882, 2021, doi: 10.1109/JIOT.2020.3016643.

[15] E. Municio, G. Daneels, M. Vucinic, S. Latré, J. Famaey, Y. Tanaka, K. Brun, K. Muraoka, X. Vilajosana, and T. Watteyne, "Simulating 6TiSCH networks," *Trans. Emerg. Telecommun. Technol.*, vol. 30, no. 3, p. e3494, 2019, doi: 10.1002/ett.3494.

[16] "IEEE standard for local and metropolitan area networks–part 15.4: Low-rate wireless personal area networks (lr-wpans) amendment 3: Physical layer (phy) specifications for low-data-rate, wireless, smart metering utility networks," *IEEE Std 802.15.4g-2012*, pp. 1–252, 2012, doi: 10.1109/JPROC.2010.2070470.

[17] M. R. Palattella, T. Watteyne, Q. Wang, K. Muraoka, N. Accettura, D. Dujovne, L. A. Grieco, and T. Engel, "On-the-fly bandwidth reservation for 6TiSCH wireless industrial networks," *IEEE Sens. J.*, vol. 16, no. 2, pp. 550–560, 2016, doi: 10.1109/JSEN.2015.2480886.

[18] A. Goldsmith, *Wireless Communications*. Cambridge University Press, 2005, isbn: 978-0521837163.

[19] "CC1352R simplelink high-performance multi-band wireless MCU," 2020, url: https://www.ti.com/lit/gpn/cc1352p.

[20] A. Elsts, "TSCH-Sim: Scaling up simulations of TSCH and 6TiSCH networks," *Sensors*, vol. 20, no. 19, 2020, doi: 10.3390/s20195663.

[21] X. Vilajosana, K. Pister, and T. Watteyne, "Minimal IPv6 over the TSCH Mode of IEEE 802.15.4e (6TiSCH) Configuration," Internet Requests for Comments, RFC 8180, May 2017, doi: https://doi.org/10.17487/RFC8180.